Prostate Cancer and Prostatic Diseases (2008) 11, 173–180
 1365-7852/08 $30.00
www.nature.com/pcan

ORIGINAL ARTICLE

Differential gene expression in the peripheral zone compared to the transition zone of the human prostate gland

EE Noel[1,4], N Ragavan[2,3,4], MJ Walsh[2], SY James[1], SS Matanhelia[3], CM Nicholson[3], Y-J Lu[1] and FL Martin[2]

[1]*Medical Oncology Centre, Institute of Cancer, Barts and London School of Medicine and Dentistry Queen Mary, University of London, London, UK;* [2]*Biomedical Sciences Unit, Department of Biological Sciences, Lancaster University, Lancaster, UK and* [3]*Lancashire Teaching Hospitals NHS Trust, Preston, UK*

Gene expression profiles may lend insight into whether prostate adenocarcinoma (CaP) predominantly occurs in the peripheral zone (PZ) compared to the transition zone (TZ). From human prostates, tissue sets consisting of PZ and TZ were isolated to investigate whether there is a differential level of gene expression between these two regions of this gland. Gene expression profiling using Affymetrix Human Genome U133 plus 2.0 arrays coupled with quantitative real-time reverse transcriptase-PCR was employed. Genes associated with neurogenesis, signal transduction, embryo implantation and cell adhesion were found to be expressed at a higher level in the PZ. Those overexpressed in the TZ were associated with neurogenesis development, signal transduction, cell motility and development. Whether such differential gene expression profiles may identify molecular mechanisms responsible for susceptibility to CaP remains to be ascertained.
Prostate Cancer and Prostatic Diseases (2008) **11,** 173–180; doi:10.1038/sj.pcan.4500997; published online 24 July 2007

Keywords: differential expression; oligonucleotide microarrays; prostate adenocarcinoma; peripheral zone; quantitative real-time RT-PCR; transition zone

Introduction

The human prostate is conventionally divided into regions or tightly fused zones known as the peripheral zone (PZ), the central zone (CZ) and the transition zone (TZ).[1] The multifocal entity of prostate adenocarcinoma (CaP) arises mostly in the PZ whereas the non-malignant overgrowth of benign prostatic hypertrophy occurs exclusively in the TZ; the CZ seems to be relatively immune to both pathologies.[1] CaP is the most common male cancer in Europe, North America and some parts of Africa,[2] and epidemiological studies of populations that migrated from low- to high-risk regions point to dietary and/or lifestyle factors playing an important role in its aetiology.[3]

CaP progression is a multistage process from latent carcinoma(s) of low-histological grade to high-grade metastatic disease.[4] Whether this pathology is predominantly PZ-associated remains to be ascertained but divergent hormone responsiveness of primary putative PZ- and TZ-derived stem cells[5] or expression of hormone-metabolising enzymes (for example, *CYP1B1*)[6] have been suggested factors in this morphological susceptibility. The CZ may have a different embryogenic origin (that is, the mesonepheric duct; the urogenital sinus is believed to give rise to the PZ and TZ[1]) and consistent with this, its protein profile differs from that of the other zones.[7] Paradoxically, PZ and TZ glandular epithelia were found to express similar protein profiles[7] and have a similar proliferative index and incidence of apoptosis.[8] Following analysis by Fourier-transform infrared microspectroscopy, TZ epithelium was unexpectedly found to be more likely to exhibit a susceptibility-to-adenocarcinoma spectral signature than PZ.[9]

If epithelial cells lining the branched tubuloacinar glands of the PZ and TZ are equally susceptible to initiating events, other effects (for example, growth promotion by hormone-associated genes or the epigenetic silencing of protective genes) might give rise to CaP progression. To investigate this, we examined the differential gene expression profile of CaP-free tissue sets consisting of PZ and TZ. Employing oligonucleotide microarrays and candidate gene verification using quantitative real-time reverse transcriptase (RT)-polymerase chain reaction (PCR), our aim was to identify genes whose zone-specific preferential expression might be associated with susceptibility or resistance to CaP.

Correspondence: Dr FL Martin, Biomedical Sciences Unit, Department of Biological Sciences, Lancaster University, Lancaster LA1 4YQ, UK.
E-mail: f.martin@lancaster.ac.uk
[4]These authors contributed equally to this study.
Received 22 January 2007; revised 7 May 2007; accepted 10 June 2007; published online 24 July 2007

Materials and methods

Study participants

Informed consent to obtain tissue for research was obtained (LREC no. 2003.6.v; Preston, Chorley and South Ribble Ethical Committee). Study participants were selected from patients undergoing radical retropubic prostatectomy (RRP) for CaP on the basis of a low prostate-specific antigen ($<20\,\mu g/l$ serum) and low volume of disease ($\leqslant 2$ core biopsies positive for CaP per 8 taken). A further CaP-free tissue was obtained after a radical cystoprostatectomy for removal of muscle-invasive bladder carcinoma.

Tissue retrieval and storage

After surgical resection, prostate tissue was transported to the pathology laboratory (<3 min) and dissected using aseptic techniques. Provisionally, tissue assumed to be cancer-free was selected (from the lobe from which biopsy cores were negative for cancer); formalin-fixed sections stained with hematoxylin and eosin were checked retrospectively to assess whether CaP was likely to be absent. Using a forceps and scalpel, the prostate tissue was sliced from the upper part of the gland starting just above the area of the verumontanum. The tissues (2 cm in length and 0.3 cm in width) isolated from the most peripheral and postero-lateral aspect of the gland were designated as PZ while the tissues (1.5 cm in length and 0.3 cm in width) isolated from the area immediately lateral to the urethra (peri-urethral) were designated as TZ. Tissue sets (PZ and TZ per individual patient) were immediately placed in RNAlater (Qiagen Ltd, Crawley, West Sussex, UK) and stored at -85°C. Remaining prostate was formalin fixed for histopathology.

Tissue sets consisting of PZ and TZ were obtained from 12 patients (53–69 years); 11 of these underwent RRP while patient 12 had a cystoprostatectomy (Table 1). On digital rectal examination, carried out by a single assessor, eight participants were characterized as benign (non-cancerous-feeling glands—stage T_1c) and the remaining patients had a malignant-feeling gland in one lobe (stage T_2). A single pathologist assigned the Gleason grade; in one tissue (PZ of patient no. 4), a node of malignancy was found following retrospective histopathology.

RNA extraction

Towards transcript profiling, total RNA was extracted using TRIzol reagent (Invitrogen, Paisley, UK) according to the manufacturer's instructions and purified by ethanol precipitation to remove any residual reagents. RNA concentration was quantified using the Nanodrop ND-1000 spectrophotometer, and quality was assessed by observing the integrity of 28S and 18S bands using an Agilent 2100 Bioanalyzer (Agilent Technologies, Waldbronn, Germany). For the purposes of this study, the samples were grouped by prostate zone. Samples ($n=6$) from three tissue sets (PZ and TZ per individual patient) were stored at -80°C until use and contributed separately (that is, one sample per chip) towards three values per prostate region (Figures 1a and b).

Towards quantitative real-time RT-PCR, total RNA extraction was performed using the Qiagen RNeasy Kit in combination with the Qiagen RNase-free DNase kit (Qiagen Ltd).

Based on experience, these two extraction methods were conducted independently in different laboratories. However, the finding that both sets of analyses were confirmatory (see below) lends strong support to the robustness of the datasets generated.

Transcript profiling and data analysis

A One Cycle Eukaryotic Target Labeling Assay (Affymetrix, Santa Clara, CA, USA) was used for amplification and biotinylation of tissue-extracted RNA. Sample preparation and hybridization were carried out following the manufacturer's instructions. Briefly, 5 μg of total RNA was reverse transcribed using T7 promoter sequence-tagged random hexamers and the resulting double-stranded cDNA was used as a template to generate biotin-labelled antisense cRNA by *in vitro* transcription. After clean-up, 20 μg of full-length cRNA was fragmented by metal-induced hydrolysis. The quality of the fragmented cRNA was verified on an Agilent 2100 Bioanalyzer (Agilent Technologies). Samples were hybridized for 16 h at 45°C on the Affymetrix Human Genome U133 plus 2.0 high-density microarray containing 54 675 probes (that is, 24 325 Unigene clusters). Following post-hybridization washes, the arrays were scanned using the Affymetrix GeneChip Scanner 3000 7G and expression data were analysed using GeneSpring v7.2 software (Silicon Genetics, Redwood

Table 1 Details of study participants and tissue samples examined

Patient no.	*Age (years)*	*PSA (μg/l)*	*DRE*	*Smoking status*	*Alcohol*	*Diet*	*Gleason grade*
1	54	4.6	T_2 right lobe	No	Yes	NV	4+3
2	68	4.4	Benign	No	Yes	NV	3+4
3	58	4.6	Benign	No	Yes	NV	3+3
4	53	19.1	T_2 right lobe	Yes	Yes	NV	4+3
5	53	8.1	T_2 left lobe	Yes	Yes	NV	3+3
6	67	8.1	Benign	No	Yes	NV	3+4
7	68	6.9	Benign	Yes	Yes	NV	3+4
8	69	8.0	Benign	Yes	Yes	NV	3+3
9	67	6.2	T_2 left lobe	Yes	Yes	NV	4+3
10	60	5.4	Benign	Yes	Yes	NV	3+3
11	59	4.4	Benign	Yes	Yes	NV	3+4
12[a]	62	9.0	Benign	Yes	Yes	NV	NA

Abbreviations: DRE, digital rectal examination; NA, not applicable; NV, non-vegetarian; PSA, prostate-specific antigen.
Gleason grade given is in reference to CaP present in the lobe from which biopsy cores were positive for cancer.
[a]All patients had RRP except patient no. 12 who had cystoprostatectomy for removal of muscle-invasive bladder carcinoma.

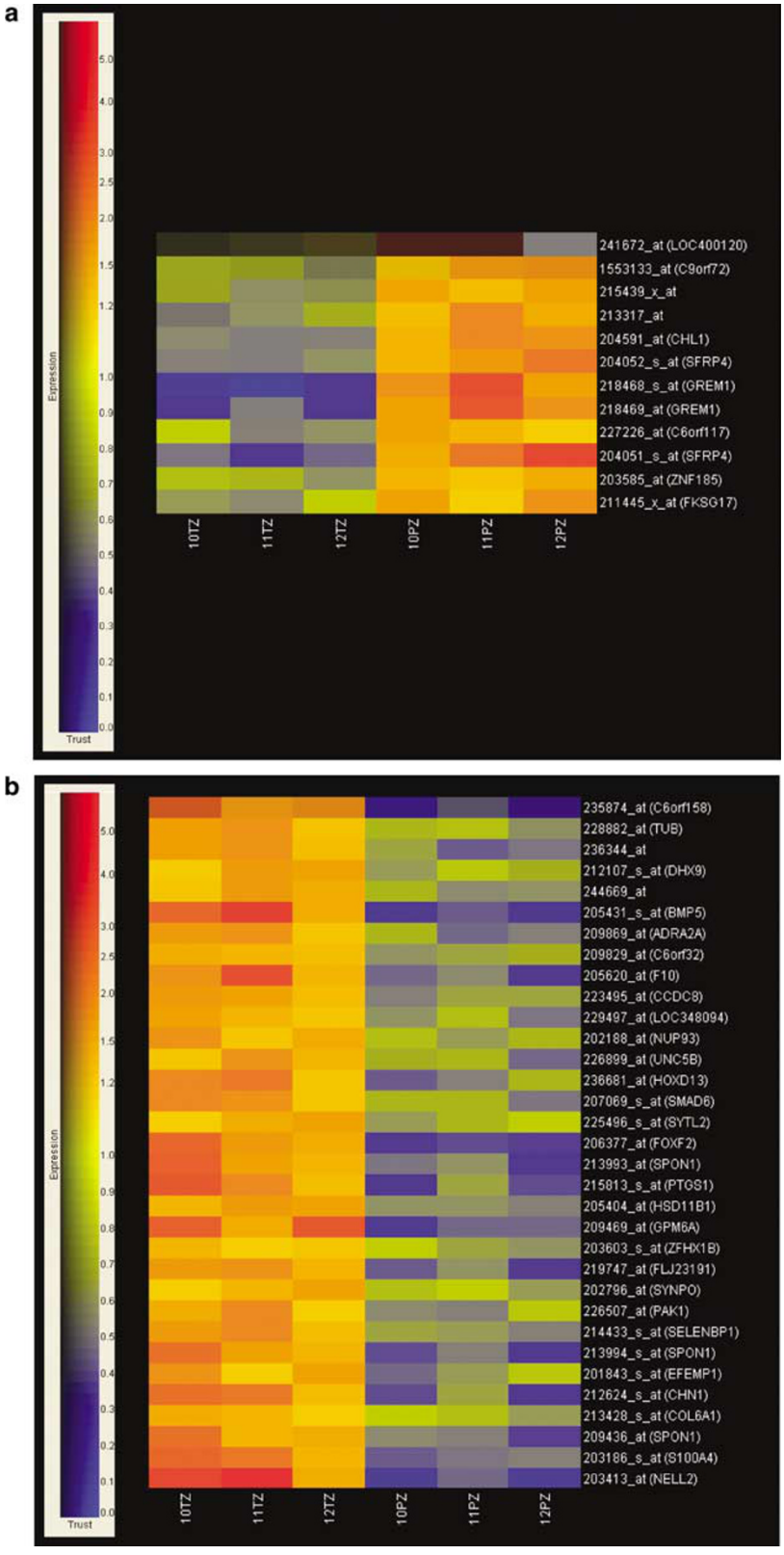

Figure 1 Preferentially expressed genes in the (**a**) PZ compared to the TZ and (**b**) TZ compared to the PZ of human prostate. A conditional tree-view of differentially expressed genes is shown in which the vertical axis corresponds to the candidate genes and the horizontal axis to the tissue samples. The colour-bar scale gives an indication of the level of expression with red representing preferentially expressed transcripts and green to blue representing lower expression. RNA samples from individual tissues contributed separately towards three values grouped by prostate zone (that is, derived from three samples applied to three different chips). Significance was set at a level of $P < 0.01$.

City, CA, USA). Raw data were normalized per chip (50th percentile) and per gene (median). A 2-fold cut-off value was set with genes filtered on flags to remove those absent in all samples and to only conserve the present and marginal-flagged genes. Statistical filtering was then applied to the remaining list; a variance analysis (one-way ANOVA test) of the expression values was performed with a level of significance set at $P < 0.01$. From the resulting list of statistically significant genes, differentially expressed (that is, between PZ and TZ per individual patient) candidate genes were identified and individually checked for consistent differential expression. Finally, ontological analysis using the Gene Ontology option available on GeneSpring v7.2 software as well as the Human Gene Nomenclature Database (www.genecards.org) was carried out to investigate the function of the selected genes and their relevance to CaP progression.

Quantitative real-time RT-PCR

RNA (0.4 μg) was reverse transcribed in a final volume of 20 μl containing Taqman reverse transcription reagents (Applied Biosystems, Warrington, Cheshire, UK): $1\times$ Taqman RT buffer; $MgCl_2$ (5.5 mM); oligo $d(T)_{16}$ (2.5 μM); dNTP mix (dGTP, dCTP, dATP and dTTP; each at a concentration of 500 μM); RNase inhibitor (0.4 U/μl); RT (MultiScribe; Applied Biosystems) (1.25 U/μl) and RNase-free water. Reaction mixtures were then incubated at 25°C (10 min), 48°C (30 min) and 95°C (5 min).

cDNA samples were stored at −20°C before use. Primers (Table 2) for candidate genes, and endogenous control *β-ACTIN* was chosen using Primer Express software 2.0 (Applied Biosystems) and designed so that one primer spanned an exon boundary. Specificity was confirmed using the NCBI BLAST search tool. Quantitative real-time PCR was performed using an ABI Prism 7000 Sequence Detection System (Applied Biosystems). Reaction mixtures contained $1\times$ SYBR Green PCR master mix (Applied Biosystems); forward and reverse primers (Invitrogen) at a concentration of 300 nM; for the candidate gene amplification 20 ng cDNA template or for *β-ACTIN* amplification 5 ng cDNA template; made to a total volume of 25 μl with sterile H_2O. Thermal cycling parameters included activation at 95°C (10 min) followed by 40 cycles each of denaturation at 95°C (15 s) and annealing/extending at 60°C (1 min). Each reaction was performed in triplicate (using the same master mix) and 'no-template' controls were included in each experiment. Dissociation curves were run to eliminate non-specific amplification, including primer-dimers.

Results

Transcript profiling in the PZ and TZ

A genome-wide approach was employed to investigate whether a differential gene expression signature associated with the PZ versus TZ of normal human prostate could be identified. For transcript profiling, three CaP-free tissues were selected (patient nos. 10, 11 and 12; see Table 1); following total RNA extraction, these samples contributed separately towards gene expression microarray analysis. By comparing tissue sets consisting of PZ and TZ, a list of genes showing differential expression between both zones was established; 45 probes representing 43 genes were identified as differentially regulated in the PZ compared to the TZ, including 33 under- and 12 overexpressed (Figures 1a and B). The majority of the differentially expressed genes were preferentially expressed in the TZ compared to PZ. Each gene was assigned to a biological process group (Table 3) based on the Gene Ontology database.

Genes preferentially expressed in the PZ compared to the TZ included bone morphogenetic protein (BMP) antagonist gremlin (*GREM1*, 7.6- to 11.6-fold difference), secreted frizzled-related protein 4 (*SFRP4*, 5.5- to 6.1-fold difference), close homologue of L1 (*CHL1*, 2.8- to 3.4-fold difference) and zinc finger protein 185 (*ZNF185*, 2.2-fold difference) (Figure 1a). Those identified to be preferentially expressed in the TZ included neural epidermal growth factor-like like 2 (*NELL2*, 10-fold difference), bone morphogenetic protein-5 (*BMP5*, 10-fold difference) and *S100A4* (5-fold difference) (Figure 1b). These fold differences ranged from 2.09 to 11.65 for preferentially expressed PZ genes and 2.01 to 11.52 for preferentially expressed TZ genes (see Supplementary Material).

Table 2 Primers used for quantitative real-time RT-PCR analyses of candidate genes

Gene	*Name*	*GenBank accession no.*	*Sequence (5′ → 3′)*
GREM1	*GREM1-F*	NM_013372	CGC CGC ACT GAC AGT ATG AG
	GREM1-R		ACC TTG GGA CCC TTT CTT TTT C
SFRP4	*SFRP4-F*	NM_003014	CCC GGA GGA TGT TAA GTG GAT
	SFRP4-R		AGG CGT TTA CAG TCA ACA TCA AGA
CHL1	*CHL1-F*	NM_006614	GGG TCA TAG CCG TGA ACG AA
	CHL1-R		TTC CTA TCT GGA GCT GCT GGT G
NELL2	*NELL2-F*	NM_006159	AAG GTA TAA TGC AAG ATG TCC AAT T
	NELL2-R		AAG TTG GAC AGG TGC GAT TAA GA
BMP5	*BMP5-F*	NM_021073	ACA GCA GCT GAA TTC CGG ATA T
	BMP5-R		CAG ATC TGC ATC CCT ATT TGT GTA TT
S100A4	*S100A4-F*	NM_019554	AGT ACG TGT GAT CCT GAC TGC TGT
	S100A4-R		GCC CGA GTA CTT GTG GAA GGT
ZNF185	*ZNF185-F*	NM_007150	GAA GAG GAC GGG CCT TCT G
	ZNF185-R		CCT CAC CTC TTG AGC TGT TTG A
β-ACTIN	*β-ACTIN-F*	AK222925	CCT GGC ACC CAG CAC AAT
	β-ACTIN-R		GCC GAT CCA CAC GGA GTA CT

Abbreviations: F, forward primer; R, reverse primer.
Nucleotide sequences were obtained from GenBank (National Center for Biotechnology Information, Bethesda, USA; http://www.ncbi.nlm.nih.gov/).

Table 3 Biological classification of genes differentially expressed between the PZ and the TZ of human prostate

Probe set ID	*Gene symbol*	*Gene title*	*Gene Ontology biological process terms*
235874_at	*C6orf158*	Chromosome 6 open reading frame 158	Proteolysis
228882_at	*TUB*	Tubby homolog (mouse)	Phototransduction; sensory perception of sound
236344_at		Transcribed sequences	
212107_s_at	*DHX9*	DEAH (Asp-Glu-Ala-His) box polypeptide 9	
244669_at		LOC389414 (LOC389414), mRNA	
205431_s_at	*BMP5*	Bone morphogenetic protein 5	Growth; skeletal development; cell differentiation
209869_at	*ADRA2A*	Adrenergic, α-2A-, receptor	Activation of MAPK; cell motility; signal transduction; G protein–coupled receptor protein signalling pathway; regulation of adenylate cyclase activity
209829_at	*C6orf32*	Chromosome 6 open reading frame 32	
205620_at	*F10*	Coagulation factor X	Blood coagulation; proteolysis and peptidolysis
223495_at	*CCDC8*	Coiled-coil domain containing 8	
229497_at	*LOC348094*	Hypothetical protein LOC348094	Signal transduction
202188_at	*NUP93*	KIAA0095 gene product	Transport
226899_at	*UNC5B*	Unc-5 homolog B (*C. elegans*)	Signal transduction; apoptosis; development
23668l_at	*HOXD13*	Homeo box D13	Skeletal development; regulation of transcription, DNA-dependent; development
207069_s_at	*SMAD6*	MAD homolog 6 (*Drosophila*)	Regulation of transcription
225496_s_at	*SYTL2*	Synaptotagmin-like protein 2	Intracellular protein and vesicle-mediated transport
206377_at	*FOXF2*	Forkhead box F2	Regulation of transcription; vasculogenesis; organ morphogenesis
213993_at	*SPON1*	Spondin 1, extracellular matrix protein	Cell adhesion; development
2158l3_s_at	*PTGS1*	Prostaglandin-endoperoxide synthase 1	Lipid metabolism; physiological process; prostaglandin biosynthesis; fatty acid biosynthesis; blood pressure regulation
205404_at	*HSD11B1*	Hydroxysteroid (11-β) dehydrogenase 1	Metabolism; steroid metabolism; lung development
209469_at	*GPM6A*	Glycoprotein M6A	X
203603_s_at	*ZFHX1B*	Zinc finger homeobox 1b	Regulation of transcription; neural crest cell migration; somitogenesis
219747_at	*FLJ23191*	Hypothetical protein FLJ23191	
202796_at	*SYNPO*	Synaptopodin	Cortical cytoskeleton organization and biogenesis
226507_at	*PAK1*	p21/Cdc42/Rac 1-activated kinase 1 (yeast)	Protein amino acid phosphorylation; Apoptosis; ER-nuclear signaling pathway; cytoskeleton organization and biogenesis; JNK cascade
214433_s_at	*SELENBP1*	Selenium-binding protein 1	Selenium binding
201843_s_at	*EFEMP1*	EGF-containing fibulin-like extracellular matrix protein 1	Visual perception
212624_s_at	*CHN1*	Chimerin (chimaerin) 1	Intracellular signalling cascade
213428_s_at	*COL6A1*	Collagen, type VI, α1	Phosphate transport; cell adhesion
203186_s_at	*S100A4*	S100 calcium binding protein A4	
203413_at	*NELL2*	NEL-like 2 (chicken)	Cell adhesion
241672_at	*LOC400120*	Hypothetical gene supported by BC036540	
1553133_at	*C9orf72*	Chromosome 9 open reading frame 72	
215439_x_at		AU146391 HEMBB1 *Homo sapiens* cDNA clone	
2133l7_at		mRNA; cDNA DKFZp564B076	
20459l_at	*CHL1*	Cell adhesion molecule with homology to L1CAM	Neuron migration; cell adhesion; signal transduction; development
204052_s_at	*SFRP4*	Secreted frizzled-related protein 4	Embryo implantation; signal transduction; cell differentiation
218468_s_at	*GREM1*	Cysteine knot superfamily 1, BMP antagonist 1	Cell-cell signaling; organ morphogenesis; development; neurogenesis
218469_at	*GREM1*	Cysteine knot superfamily 1, BMP antagonist 1	Cell-cell signaling; organ morphogenesis; development; neurogenesis
227226_at	*C6orf117*	Chromosome 6 open reading frame 117	
204051_s_at	*SFRP4*	Secreted frizzled-related protein 4	Embryo implantation; signal transduction; cell differentiation
203585_at	*ZNF185*	Zinc finger protein 185 (LIM domain)	
211445_x_at	*FKSG17*	Nascent polypeptide-associated complex subunit α	Transcription; translation; protein transport

Differentially expressed (that is, between PZ and TZ per individual patient) candidate genes were identified and individually checked for consistent differential expression. Ontological analysis using the Gene Ontology option available on GeneSpring v7.2 software as well as the Human Gene Nomenclature Database (www.genecards.org) was then carried out.

Verification of differential candidate gene expression in the human prostate

Quantitative real-time RT-PCR was employed to verify the differential gene expression of four candidate genes (*GREM1*, *SFRP4*, *CHL1* and *ZNF185*) preferentially expressed in the PZ compared to TZ and three (*NELL2*, *BMP5* and *S100A4*) in the TZ (Table 4). Averaged threshold cycle (C_T) values of amplified cDNA were in the 27–35 range for *GREM1*, 24–30 for *SFRP4*, 28–35 for *CHL1*, 31–38 for *ZNF185*, 25–33 for *NELL2*, 24–36 for *BMP5* and 21–26 for *S100A4* (data not shown). Except for a small proportion of samples, inter-individual

Table 4 Relative quantitative expression in prostate zones by real-time RT-PCR

Patient no. (zone)	*Inter-individual gene expression*							*Intra-individual gene expression*							*Tissue status*
	GREM1	*SFRP4*	*CHL1*	*ZNF185*	*NELL2*	*BMP5*	*S100A4*	*GREM1*	*SFRP4*	*CHL1*	*ZNF185*	*NELL2*	*BMP5*	*S100A4*	
1 (Transition)	1 (c)	1 (c)	1 (c)	1 (c)	1 (c)	1 (c)	1 (c)	1 (c)	1 (c)	1 (c)	1 (c)	1 (c)	1 (c)	1 (c)	Cancer free
(Peripheral)	1 (c)	1 (c)	1 (c)	1 (c)	1 (c)	1 (c)	1 (c)	9.93	11.51	2.49	5.07	0.07	0.03	0.31	Cancer free
2 (Transition)	0.59	1.49	0.30	0.45	0.45	1.29	1.12	1 (c)	1 (c)	1 (c)	1 (c)	1 (c)	1 (c)	1 (c)	Cancer free
(Peripheral)	0.24	0.31	0.49	0.39	1.22	0.22	0.44	4.03	2.39	4.13	4.39	0.19	0.01	0.12	Cancer free
3 (Transition)	5.22	6.71	0.31	0.80	0.16	0.66	0.61	1 (c)	1 (c)	1 (c)	1 (c)	1 (c)	1 (c)	1 (c)	Cancer free
(Peripheral)	1.30	2.26	0.69	0.54	0.76	1.83	0.69	2.47	3.88	5.59	3.44	0.33	0.09	0.35	Cancer free
4 (Transition)	1 (c)	1 (c)	1 (c)	1 (c)	1 (c)	1 (c)	1 (c)	1 (c)	1 (c)	1 (c)	1 (c)	1 (c)	1 (c)	1 (c)	Cancer free
(Peripheral)	1 (c)	1 (c)	1 (c)	1 (c)	1 (c)	1 (c)	1 (c)	2.28	1.78	4.32	1.47	0.36	0.11	0.31	Tumour
5 (Transition)	1.36	0.63	1.05	1.22	7.71	4.03	2.4	1 (c)	1 (c)	1 (c)	1 (c)	1 (c)	1 (c)	1 (c)	Cancer free
(Peripheral)	0.49	1.55	0.53	0.47	0.63	0.94	1.88	0.82	4.40	2.19	0.57	0.03	0.03	0.24	Cancer free
6 (Transition)	2.15	0.66	1.38	0.48	0.18	0.09	1.01	1 (c)	1 (c)	1 (c)	1 (c)	1 (c)	1 (c)	1 (c)	Cancer free
(Peripheral)	1.93	0.57	2.50	1.20	1.05	0.42	1.09	2.04	1.54	7.84	3.65	2.17	0.48	0.33	Cancer free
7 (Transition)	1 (c)	1 (c)	1 (c)	1 (c)	1 (c)	1 (c)	1 (c)	1 (c)	1 (c)	1 (c)	1 (c)	1 (c)	1 (c)	1 (c)	Cancer free
(Peripheral)	1 (c)	1 (c)	1 (c)	1 (c)	1 (c)	1 (c)	1 (c)	62.61	3.01	1.91	2.94	0.10	0.01	0.26	Cancer free
8 (Transition)	1.56	0.65	0.66	0.69	1.23	0.72	1.39	1 (c)	1 (c)	1 (c)	1 (c)	1 (c)	1 (c)	1 (c)	Cancer free
(Peripheral)	1.18	1.34	1.06	0.32	2.43	2.36	1.38	47.51	6.21	3.04	1.34	0.20	0.04	0.26	Cancer free
9 (Transition)	18.61	0.89	1.15	2.40	0.81	0.74	0.90	1 (c)	1 (c)	1 (c)	1 (c)	1 (c)	1 (c)	1 (c)	Cancer free
(Peripheral)	0.94	0.79	0.54	1.23	0.61	0.76	1.14	3.15	2.69	0.90	1.51	0.07	0.01	0.34	Cancer free
10 (Transition)	1 (c)	1 (c)	1 (c)	1 (c)	1 (c)	1 (c)	1 (c)	1 (c)	1 (c)	1 (c)	1 (c)	1 (c)	1 (c)	1 (c)	Cancer free
(Peripheral)	1 (c)	1 (c)	1 (c)	1 (c)	1 (c)	1 (c)	1 (c)	21.31	4.76	8.92	36.17	0.13	0.00	0.10	Cancer free
11 (Transition)	0.31	0.56	0.70	1.67	5.19	1.71	0.74	1 (c)	1 (c)	1 (c)	1 (c)	1 (c)	1 (c)	1 (c)	Cancer free
(Peripheral)	0.22	0.35	0.45	0.04	6.77	1230.48	3.95	14.59	2.94	5.70	0.94	0.17	0.35	0.55	Cancer free
12 (Transition)[a]	7.73	2.65	2.78	3.18	0.58	0.54	0.60	1 (c)	1 (c)	1 (c)	1 (c)	1 (c)	1 (c)	1 (c)	Cancer free
(Peripheral)	0.52	1.86	1.25	0.43	0.94	37.75	1.73	1.42	3.34	4.02	4.88	0.21	0.03	0.30	Cancer free

Reactions were performed in triplicate and 'no-template' controls were included. Averaged threshold cycle (C_T) values for each reaction were normalized to *β-ACTIN* values thus giving ΔC_T values. Alterations in gene expression were determined by comparison with the calibrator or (c), giving $\Delta\Delta C_T$ values. Relative gene expression was calculated using the formula $2^{-\Delta\Delta C_T}$. Levels of mRNA transcripts were compared in tissue sets from groups of three patients per experiment. For inter-individual variations, the mRNA transcript levels in peripheral zone or transition zone derived from the first patient number was arbitrarily taken as the calibrator. For intra-individual variations, an mRNA transcript level in transition zone for each individual tissue set was taken as the calibrator.

[a]All patients had RRP except patient no. 12 who had cystoprostatectomy for removal of muscle-invasive bladder carcinoma.

variations in candidate gene expression were not marked. Preferential expression in PZ compared to TZ of *GREM1* (2- to 62-fold, except for two tissue sets), *SFRP4* (2- to 11-fold, except for a separate two tissue sets), *CHL1* (2- to 9-fold, except for yet another tissue set) and *ZNF185* (2- to 36-fold, except for five tissue sets) was observed (Table 4). In comparison, lower expression in the PZ compared to the TZ of *NELL2* (2- to 33-fold, except for one tissue set), *BMP5* (2- to 100-fold) and *S100A4* (2- to 10-fold) was verified (Table 4).

Discussion

Although morphologically similar,[8] it remains unknown whether there is a specific underlying mechanism that may confer susceptibility to CaP progression in the PZ or, conversely, resistance in the TZ in normal human prostate.[10] Prostatic glandular tissue possesses the metabolic machinery to activate pro-carcinogens or hormones to DNA-reactive electrophilic species,[6,11] and such agents induce measurable levels of damage in isolated primary prostate epithelial cells.[12] For this study, stringent attempts were made to isolate and examine CaP-free tissues but given the age range of the participants (53–69 years) and the fact that most were undergoing RRP for organ-confined disease, there was always a distinct possibility that disease-progressive changes were present even though they may not be observable by histology. However, an advantage of this approach would be that gene expression profiles responsible for disease progression may be present that would be absent in tissues isolated from a younger cohort.[13]

Genes preferentially expressed in the PZ were associated with neurogenesis development (*GREM1* initiates epithelial–mesenchymal signalling interactions during organogenesis), signal transduction (*SFRP4* is a negative regulator of Wnt signalling), embryo implantation and cell adhesion (*CHL1* promotes cell migration, axonal growth and synaptic remodelling) (Table 3). *GREM1*-mediated expression is essential to initiate epithelial–mesenchymal signalling interactions during embryonic organogenesis.[14] BMP is a potential regulator of ureter development and antagonism by *GREM1* expression may confer survival advantages. SFRP proteins bind directly to Wnt ligands and methylation silencing of *SFRP4* may play important roles in aberrant Wnt activation.[15] *CHL1*, located on human chromosome 3p26.1, is expressed in neurons and glia of both the central and peripheral nervous system, and promotes neurite outgrowth and neuronal survival; its role may be in integrin-dependent cell migration.[16] Methylation-

specific PCR has shown *ZNF185* inactivation by cytosine-phosphate-guanine dinucleotide methylation suggesting that epigenetic alterations resulting in transcriptional silencing may be a useful biomarker of CaP progression.[17] Recent studies suggest that ZNF185 may function as a tumour-suppressor protein by associating with the actin cytoskeleton through its N-terminal region.[18] Our findings suggest that *ZNF185* overexpression may be an important block to CaP progression in the PZ and its epigenetic inactivation may remove this protection.

Those genes preferentially expressed in the TZ were associated with neurogenesis, signal transduction (*NELL2* may promote survival through modulation on mitogen-activated protein kinases (MAPKs)), cell motility (the S100 calcium-binding protein of *S100A4*) and development (BMPs of *BMP-5* are secreted signalling proteins that induce ecotopic bone) (Table 3). *NELL2* appears to promote neuronal survival by modulating MAPKs and consequently is highly expressed in hippocampus and cerebral cortex; its gene product is a thrombospondin-1-like protein exhibiting six epidermal growth factor-like domains,[19] most probably acting as a multi-domain adhesive in the extracellular matrix and participating in cell–cell communication.[20] In the central nervous system, *NELL2* is expressed in nascent, post-mitotic neurons as they start to differentiate whereas, in the peripheral nervous system, it is also expressed in subsets of progenitor cells.[20] *BMP5* may be expressed early in skeletal development and local expression may prefigure specific anatomical structures in the vertebrate skeleton.[21] It may also play a role in the control of apoptosis during limb development with Smad proteins and MAPK p38 acting as intracellular effectors.[22] *S100A4* overexpression has been associated with cancer (including CaP) progression, invasion and metastasis; its gene product is a member of the S100 calcium-binding protein family whose upregulation is inversely correlated with E-cadherin expression.[23]

A check of exon results consisting of Affymetrix array data for the LNCaP, DU-145, PC-3 and 22RV1 prostate cancer cell lines and one primary sample (unpublished data, Medical Oncology Centre, Institute of Cancer, University of London) was conducted. From this dataset a number of the genes (*CCDC8*, *HOXD13*, *SPON1*, *PTGS1*, *HSD11B1*, *ZFHX1B*, *SYNPO*, *UNC5B*, *S100A4*) observed to be overexpressed in normal TZ tissues, which were hitherto identified to be downregulated in prostate cancer cells and CaP tissues, were noted.[24–27] No genes preferentially expressed in normal PZ tissues were noted on the exon array (unpublished data). However, *SFRP4* was actually downregulated in the exon array but the literature reports that this is overexpressed in CaP.[28]

Marked differences in intra-individual gene expression patterns in the PZ compared to the TZ were observed (Table 4). Of note was the observation that many of these differentially expressed genes have previously been associated with cell growth and division, differentiation and cell migration. The expression patterns of these genes may result in an environment favouring zone-specific susceptibility or resistance to CaP progression. Alternatively, alterations of such gene expression profiles (for example, through transcriptional silencing) may be the pivotal pre- or post-initiation events.

Acknowledgements

We thank Tracy Chaplin for technical support with the array processing. This work was funded by Rosemere Cancer Foundation (NR, MJW and FLM), Orchid Cancer Appeal (EN, SJ and Y-JL) and Cancer Research UK (Tracy Chaplin).

References

1 McNeal JE. The prostate gland: morphology and pathobiology. *Monograph Urol* 1988; **9**: 36–63.
2 Parkin DM, Bray F, Ferlay J, Pisani P. Global Cancer Statistics, 2002. *CA Cancer J Clin* 2005; **55**: 74–108.
3 Grover PL, Martin FL. The initiation of breast and prostate cancer. *Carcinogenesis* 2002; **23**: 1095–1102.
4 Grönberg H. Prostate cancer epidemiology. *Lancet* 2003; **361**: 859–864.
5 Kirschenbaum A, Liu XH, Yao S, Narla G, Friedman SL, Martignetti JA *et al*. Sex steroids have differential effects on growth and gene expression in primary human prostatic epithelial cell cultures derived from the peripheral versus transition zones. *Carcinogenesis* 2006; **27**: 216–224; doi:10.1093/carcin/bgi219.
6 Ragavan N, Hewitt R, Cooper LJ, Ashton KM, Hindley AC, Nicholson CM *et al*. *CYP1B1* expression in prostate is higher in the peripheral than in the transition zone. *Cancer Lett* 2004; **215**: 69–78.
7 Lexander H, Franzén B, Hirschberg D, Becker S, Hellström M, Bergman T *et al*. Differential protein expression in anatomical zones of the prostate. *Proteomics* 2005; **5**: 2570–2576.
8 Laczkó I, Hudson DL, Freeman A, Feneley MR, Masters JR. Comparison of the zones of the human prostate with the seminal vesicle: morphology, immunohistochemistry, and cell kinetics. *Prostate* 2005; **62**: 260–266.
9 German MJ, Hammiche A, Ragavan N, Tobin MJ, Fullwood NJ, Matanhelia SS *et al*. Infrared spectroscopy with multivariate analysis potentially facilitates the segregation of different types of prostate cell. *Biophys J* 2006; **90**: 3783–3795.
10 van der Heul-Nieuwenhuijsen L, Hendriksen PJM, van der Kwast TH, Jenster G. Gene expression profiling on the human prostate zones. *BJU Int* 2006; **98**: 886–897.
11 Williams JA, Martin FL, Muir GH, Grover PL, Phillips DH. Metabolic activation of carcinogens and expression of various cytochromes P450 in human prostate tissue. *Carcinogenesis* 2000; **21**: 1683–1689.
12 Martin FL, Cole KJ, Muir GH, Kooiman GG, Williams JA, Sherwood RA *et al*. Primary cultures of prostate cells and their ability to activate carcinogens. *Prostate Cancer Prostatic Dis* 2002; **5**: 96–104.
13 Daly-Burns B, Alam TN, Mackay A, Clark J, Shepherd CJ, Rizzo S *et al*. A conditionally immortalized cell line model for the study of human prostatic epithelial cell differentiation. *Differentiation* 2007; **75**: 35–48.
14 Michos O, Panman L, Vintersten K, Beier K, Zeller R, Zuniga A. *Gremlin*-mediated BMP antagonism induces the epithelial-mesenchymal feedback signaling controlling metanephric kidney and limb organogenesis. *Development* 2004; **131**: 3401–3410.
15 He B, Lee AY, Dadfarmay S, You L, Xu Z, Reguart N *et al*. Secreted frizzled-related protein 4 is silenced by hypermethylation and induces apoptosis in β-catenin-deficient human mesothelioma cells. *Cancer Res* 2005; **65**: 743–748.
16 Buhusi M, Midkiff BR, Gates AM, Richter M, Schachner M, Maness PF. Close homolog of L1 is an enhancer of integrin-mediated cell migration. *J Biol Chem* 2003; **278**: 25024–25031.
17 Vanaja DK, Cheville JC, Iturria SJ, Young CYF. Transcriptional silencing of zinc finger protein 185 identified by expression profiling is associated with prostate cancer progression. *Cancer Res* 2003; **63**: 3877–3882.

18 Zhang J-S, Gong A, Young CYF. ZNF185, an actin-cytoskeleton-associated growth inhibitory LIM protein in prostate cancer. *Oncogene* 2007; **26**: 111–122.
19 Aihara K, Kuroda S, Kanayama N, Matsuyama S, Tanizawa K, Horie M. A neuron-specific EGF family protein, NELL2, promotes survival or neurons through mitogen-activated protein kinases. *Mol Brain Res* 2003; **116**: 86–93.
20 Nelson BR, Matsuhashi S, Lefcort F. Restricted neural epidermal growth factor-like like 2 (*NELL2*) expression during muscle and neuronal differentiation. *Mech Dev* 2002; **119S**: S11–S19.
21 DiLeone RJ, Marcus GA, Johnson MD, Kingsley DM. Efficient studies of long-distance *Bmp5* gene regulation using bacterial artificial chromosomes. *Proc Natl Acad Sci USA* 2000; **97**: 1612–1617.
22 Zuzarte V, Montero JA, Rodriguez-Leon J, Merino R, Rodrigues JC, Hurle JM. A new role for BMP5 during limb development acting through synergic activation of Smad and MAPK pathways. *Dev Biol* 2004; **272**: 39–52.
23 Saleem M, Adhami VM, Ahmad N, Gupta S, Mukhtar H. Prognostic significance of metastasis-associated protein S100A4 (Mts1) in prostate cancer progression and chemoprevention regimens in an autochthonous mouse model. *Clin Cancer Res* 2005; **11**: 147–153.
24 Žbánková Š, Bryndová J, Kment M, Pácha J. Expression of 11β-hydroxysteroid dehydrogenase types 1 and 2 in colorectal cancer. *Cancer Lett* 2004; **210**: 95–100.
25 Comijn J, Berx G, Vermassen P, Verschueren K, van Grunsven L, Bruyneel E *et al*. The two-handed E box binding zinc finger protein SIP1 downregulates E-cadherin and induces invasion. *Mol Cell* 2001; **7**: 1267–1278.
26 Thiébault K, Mazelin L, Pays L, Llambi F, Joly M-O, Scoazec J-Y *et al*. The netrin-1 receptors UNC5H are putative tumor suppressors controlling cell death commitment. *Proc Natl Acad Sci USA* 2003; **100**: 4173–4178.
27 Gupta S, Hussain T, MacLennan GT, Fu P, Patel J, Mukhtar H. Differential expression of *S100A2* and *S100A4* during progression of human prostate adenocarcinoma. *J Clin Oncol* 2003; **21**: 106–112.
28 Horvath LG, Henshall SM, Kench JG, Saunders DN, Lee C-S, Golovsky D *et al*. Membranous expression of secreted frizzled-related protein 4 predicts for good prognosis in localized prostate cancer and inhibits PC3 cellular proliferation *in vitro*. *Clin Cancer Res* 2004; **10**: 615–625.

Supplementary Information accompanies the paper on the Prostate Cancer and Prostatic Diseases website (http://www.nature.com/pcan)